Rotational particle separator : an efficient method to separate micron-sized droplets and particles from fluids

ROTATIONAL PARTICLE SEPARATOR: AN EFFICIENT METHOD TO SEPARATE MICRON-SIZED DROPLETS AND PARTICLES FROM FLUIDS

J.J.H. Brouwers*, H.P. van Kemenade, J.P. Kroes

Eindhoven University of Technology
P.O. Box 513
5600MB Eindhoven, the Netherlands
j.j.h.brouwers@tue.nl
www.tue.nl/ptc

Abstract

The rotational particle separator (RPS) has a cyclone type house within which a rotating cylinder is placed. The rotating cylinder is an assembly of a large number of axially oriented channels, e.g. small diameter pipes. Micron-sized particles entrained in the fluid flowing through the channels are centrifugated towards the walls of the channels. Here they form a layer or film of particles material which is removed by applying pressure pulses or by flowing of the film itself. Compared to conventional cyclones the RPS is an order of magnitude smaller in size at equal separation performance, while at equal size it separates particles ten times smaller. Applications of the RPS considered are: ash removal from hot flue gases in small scale combustion installations, product recovery in stainless environment for pharma/food, oil water separation and demisting of gases. Elementary formulae for separation performance are presented and compared with measurements performed with various RPS design.

1 Introduction

Many processes require the separation of micron sized particles from a gas stream. Techniques employed to do the job are: scrubbers, fabric filters, electrostatic separators, and (multi-)cyclones. There is still a drive however to develop new technologies: scrubbers are sizeable and fail to remove micron-sized particles, fabric filters and electrostatic precipitators are limited to dry and/or chargeable particulate matter and involve large installations, and cyclones in industrial installations subject to large volume flows fail to collect micron sized particles [1]. A new development which overcomes several of the aforementioned limitations is the rotational particle separator, in short RPS [2]. The RPS has a cyclone type house within which a rotating cylinder is placed. The rotating cylinder is an assembly of a large number of axially oriented channels. These channels provide the means to collect micron sized particles at limited rotational speed, pressure drop and short residence time (small building volume).

In this paper we show the advantage of the RPS by comparing its performance with that of vane type separators and cyclones (§2). In §3 these considerations are substantiated by results of experiments. Many RPS devices have been designed and tested over the years and in section 4 to 6 the lessons learned concerning flow stability, power consumption and loading/removal are discussed. §7 and §8 give an overview of the designs that have been realized, while in §9 the most recent design, a gas scrubber for large volume operations is treated in more detail.

2 Elementary separation: vane-type separator, cyclone and RPS

We shall compare the separative performance of devices in which separation is the result of inertial or centrifugal forces acting on particles with different density compared to that of the fluid in which they are immersed.

The vane type separator is represented by a flow through a single bend (figure 1). Three forces act on a particle moving along a curved trajectory with radius r and velocity v_θ: the centrifugal force F_c, a drag force F_d and a buoyancy force F_{buo}: $F_c = F_d + F_{buo}$. For particles with diameters ranging from about 0.5 micron to 25 micron, the fluid force can be described by Stokes flow. For smaller and larger particles Cunningham and Reynolds number corrections have to be introduced, respectively, however, at a diameter of 1 μm, the effect is only ca. 10%, omitting it is a more conservative approach [1]. The radial migration velocity of a particle can then be described as

$$v_{TC} = \frac{(\rho_p - \rho_F) d_p^2 v_t^2}{18 \mu r} \tag{1}$$

ρ_p and ρ_F are the densities of the particle respectively the carrier fluid. μ denotes the dynamic viscosity of the carrier fluid and v_t the tangential velocity.

We can now turn our attention to the collection efficiency. The trajectory of a

particle can be described as $dr/d\theta = rV_{TC}(r)/v_{ax}$ with the assumptions that the velocity of the fluid v_{ax} is uniform, no secondary flows and a tangential particle velocity equal to the carrier fluid velocity v_{ax}. Integration gives

$$r(\theta) = r(0) + \frac{(\rho_p - \rho_F)d_p^2 v_{ax}}{18\mu}\theta \tag{2}$$

where r and θ are the radial and angular position. With the assumption that the particles are uniformly distributed over the cross section when entering the separation device, the efficiency of the separator can be derived as

$$\varepsilon = \frac{r(\theta_{sep}) - r_i}{r_o - r_i} = \frac{(\rho_p - \rho_f)d_p^2 v_{ax}}{18\mu(r_o - r_i)}\theta_{sep} \tag{3}$$

θ_{sep} denotes the angle of the bend and r_o and r_i are the outer and inner radius. We can now determine the particle size that can be separated with 50 % efficiency ($\varepsilon = 0.5$) as

$$d_{p50} = \sqrt{\frac{9\mu d_c}{(\rho_p - \rho_F)v_{ax}\theta_{sep}}} \tag{4}$$

with the channel height $d_c = r_o - r_i$. In practice the minimum channel height is restricted to about a millimeter. The velocity is limited by liquid entrainment and droplet break-up. Typical values are below 10 ms^{-1}. For air-water under ambient pressure, this corresponds to a minimal d_{p50} value in the order of 10 micrometer.

The axial cyclone consists of a stationary cylindrical pipe which contains at the entrance stationary vanes or blades: figure 2. Fluid which enters the pipe and passes through these blades attains a swirling motion. Dispersed phase entrained in the fluid acquires this swirling motion as well. Having a density which is higher than the density of the carrier fluid, the dispersed phase will be subjected to a centrifugal force which causes it to move radially toward the cylindrical wall. It leaves the device via outlets so situated at the end of the pipe constituting the axial cyclone. Using a method analogous to the derivation of eq. (4), an expression for the d_{p50} is given in [3]:

$$d_{p50} = \sqrt{\frac{9\mu v_{ax} R^2}{2(\rho_p - \rho_f)v_t^2 L}} \tag{5}$$

v_t is the tangential velocity , L the length of the cyclone and R the radius. To derive this equation it is assumed that the axial velocity v_{ax} is constant over the radius.

Typical cyclones have a swirl ratio $S = v_t/v_{ax}$ of 1 to 2 and a L/R of about 5. The axial velocity can be higher compared to the vane type: in the order of 20 ms^{-1}. The only free parameter is now the radius: ie to achieve a d_{p50} of 10 micrometer the radius has to be below 0.15 m. For higher volume flows multi cyclones have to be used.

The inline version of the rotational particle separator (RPS) is an axial cyclone within which a rotating separation element is built, figure 3. The rotating element consists of a multitude of axially oriented channels of diameter of about 1 to 2 mm. The separation process taking place in the channels of the RPS is similar to that in the cyclone. In this case we can derive for d_{p50} [1]

$$d_{p50\%} = \sqrt{\frac{27\mu v_{ax} d_c R}{2(\rho_p - \rho_f) v_t^2 L}} \tag{6}$$

We can now compare the performance of the RPS to the vane separator by looking at the ratio of d_{p50} for the same axial velocities

$$\frac{d_{p50,vane}}{d_{p50,RPS}} = \sqrt{\frac{36}{27}\frac{1}{\theta_{sep}}\frac{L}{R}S^2} \tag{7}$$

While the separation angle is limited to about $\theta_{sep} = \pi/2$, the ratios R/L and $S = v_t/v_{ax}$ can be used for the RPS to increase performance.

The d_{p50} of the cyclone compares to the d_{p50} of the RPS as

$$\frac{d_{p,50cyc}}{d_{p50,RPS}} = \sqrt{\frac{R}{3d_c}} \tag{8}$$

Figure 4 depicts the d_{p50} under atmospheric pressure as a function of the volume flow $Q = \pi R^2$. The d_{p50} of the RPS remains constant below 1 micrometer, while the cyclone d_{p50} quickly rises into the micrometer range. The rotational particle separator is able to separate an order of magnitude smaller particles than the axial cyclone is able to at equal flow and dimensions.

For equal separation performance we find the relation

$$\frac{R_{cyclone}}{R_{RPS}} = \sqrt{\frac{d_c}{3R_{cyclone}}} \tag{9}$$

This ratio is a measure for the difference in footprint or space between the cyclone and RPS for an equal separation performance. For the same separation performance, the size of the RPS can be an order lower compared to a cyclone.

3 Experiments

Two measurement methods were used to assess the performance of centrifugal separators: laser diffraction and impactation. Laser diffraction is based on the phenomenon that particles illuminates by a laser beam scatter light at angles that are inversely proportional to the size of the particles. Large particles scatter at small forward angles while small particles scatter light at wider angles. Mie theory is used to establish the relation between the scattered energy distribution on the detectors and the particle size distribution. In both cases the measurement set-up is such that

the droplet distribution of a nozzle can be measured with and without the separator in place. If the nozzle droplet distribution overlaps the separator cut-off, the separator efficiency as function of the size can be deduced from both droplet distributions. The other apparatus used is a Anderson type cascade impactor whereby particles within a size class are collected on a specific stage of the impactor

3.1 Moisture separation panel

As representative for bend-type separators, we used a moisture separation panel as applied to the inlet of turbo machinery. Based on the fixed dimensions of the laser diffraction device, a square test duct with external dimensions of 220 mm was used to guide the air and droplets to the water droplet panels and through a Malvern Mastersizer S (Figure 5). Complying to standard installation, a fan was installed downstream the duct. The laser measurement is located about 300 mm downstream the outlet of the water droplet catcher panels to have sufficient mixing downstream the separator panel without significant evaporation of the droplets. Adapter pieces were constructed to allow both vertical and 15° installation. Before each spray spectrum measurement is done, the setting of the fan is checked by measuring the velocity in the middle of the duct with a hot wire measuring device. Analysis of the moisture separator panels was done at 3 ms^{-1} and 5 ms^{-1}.

A typical measurement result is depicted in figure 6. Each datapoint represents three measurements of both the nozzle distribution and the distribution after the separator. Curve (1) is the measured droplet volume distribution without a separator in the duct. Curve (2) is measured with the separator mounted between the nozzle and the measuring spot. Curve (3) is curve (2) scaled to curve (1) using the measured concentration. The probability P that a particle of a certain diameter passes through the separator is found by dividing the values of curve (3) by those of curve (2). The efficiency is equal to the probability that a particle is caught in the separator or $\varepsilon = 1 - P$. Conventionally the cut-off diameter of a separator is characterized by the diameter d_{p50} of the particle that has a 50% probability of passing through the separator, 22 μm in the case of figure 6.

The measured efficiencies scaled to their respective d_{p50} are presented in figure 7. The three panel types have slightly different geometries but all panels essentially depend on two bends for the removal of droplets. Consequently the curves overlap each other despite their difference in d_{p50}. The exception is panel type 3 at the higher velocity of 5 ms^{-1}, here re-entrainment or flooding occurs, a phenomenon reported in literature since 1939 [4]. It can be concluded that the d_{p50} indeed is a good measure to compare the performance of geometrically similar moisture panels as the efficiency distribution hardly changes.

3.2 Cyclone

The demisting stage of advanced gas-liquid scrubber vessels usually consists of a

bank of axial cyclones (swirl tubes), working in parallel. We measured the efficiency of a single commercial swirl tube in the way explained in the previous section. Since the droplets leaving the cyclone are in the range 1-10 micron, the lens of Malvern's Mastersizer S was too small; instead we used the Spraytec.

During measurements the cyclone was contained in a bigger pipe (diameter 200 mm), simulating a scrubber vessel with upwards gas flow. Nozzles injected a constant amount of water into an adjustable airflow. Droplet distributions and concentrations were measured in the open outflow above this pipe. The efficiency is determined taking a dummy cyclone (without swirl element, i.e. vanes and body removed) as reference. Measurements were done at 11 flowrates, for which the corresponding values of d_{p50} according to eq. (5) are shown in figure 8. Figure 9 shows the combined result of all measured efficiency curves.

Since all 11 curves fall virtually on one line, we can conclude that d_{p50} accounts correctly for the flowrate (velocity). The right end tail also corresponds with the prediction. We can therefore also conclude that the `cut' of the cyclone is determined by centrifugal separation, upon which the model is based. The fact that the measured curve is above theory indicates that the flow in and around the swirl element provides additional separation, for which the model does not account. Instead of providing a sharp `cut', this additional separation mechanism seems to lower the distribution as a whole.

We have to remark that despite the fact that the mist separation efficiency was conform expectations, or even somewhat better, the performance with regard to big droplets (> 200 μm) was inferior, resulting in a low overall efficiency (75% at the design load). The higher the gas velocity, the larger the volume of large droplets that we measured in the flow leaving the cyclone. The reason is that the centrifugal force goes to zero at the stationary wall, which easily leads to re-entrainment. Since the RPS has a *rotating* collection wall, it does not suffer from this problem.

3.3 RPS

Many RPS devices have been designed and tested over the past 15 years [5, 6, 7] e.g. ash removal from flue gas of combustion installations, air cleaning in domestic appliances, product recovery in pharmaceutical and food industry and oil/water separation.

Separation efficiencies have been assessed for a number of separation elements of different size (length, radius, channel, height, etc.) subject to different conditions (angular speed, flow rate, particulate matter, etc.) [7, 12, 13]. Particle collection efficiencies were determined by measuring distributions at inlet and outlet using cascade impactors and laser particle counter techniques. For each of the cases the value of d_{p50} according to equation (6) was calculated: dp_{50} varied from a value as small as 0.1 μm to 3 μm. The values of d_{p50} were subsequently used to generate separation efficiency distributions as a function of dimensionless particle diameter. Results are shown in figure 10. For reasons of comparison the theoretical curve is

shown as well. It is seen that results of measurements are consistent with each other and compare sufficiently well with theory for design purposes.

4 Flow stability

Although at first glance simple and straightforward the radial motion of phases and particles in a channel is a subtle and sensitive process. The smallest fractions aimed of being separated are those which move with a radial velocity which compares to the axial fluid velocity as the ratio of channel height to channel length as implied by equation (6). In practical applications of the rotational particle separator this ratio is very small, typically < 0.01. So smallest separated fractions move with radial velocities which are only one percent of the axial fluid velocity. If now secondary fluid flows occur in planes perpendicular to the axial channel axis which are only one percent in magnitude of the axial fluid velocity, the process of radial migration of the smallest separated fraction may already be disturbed.

Usually, the flow in the channels of the filter element is kept in the laminar regime to prevent capture of particles or droplets in turbulent eddies or swirls. In case of large volume and or high pressure applications the laminar flow condition may impose a too severe restriction on the design.

In most cases the Reynolds number is low enough for the flow and particle behaviour to be studied in detail by means of direct numerical simulation of the fluid flow and Lagrangian particle tracking [12, 13]. The results of the fluid flow show that an axial vortex is present in the flow, caused by the rotation, but also that this vortex hardly influences the collection efficiency. However, turbulent velocity fluctuations have a negative influence on the collection efficiency, especially for larger particles (figure 11). In order to meet design criteria in practice, the length of the RPS should be chosen about 20% larger than laminar design criteria prescribe to obtain the same collection efficiency. The results confirm that when the rotational particle separator is used as a bulk separator and a strictly defined cut-off diameter is not required, the working range can be extended in the turbulent range to enhance the throughput within the same volume constraints. This is a major advantage in offshore applications where platform space and load capacity are at premium and recent designs of the RPS for natural gas treatment [3,6], are operating in the turbulent regime.

Unwanted secondary flows can also occur in case the symmetry axis of a channel makes an angle with respect to the rotation axis: For example, by fabrication inaccuracy the channels can be twisted around the symmetry axis of the filter element, or they can diverge or converge as their distance from the axis of the filter element increases (or decreases) in axial direction. Coriolis forces will act on the fluid as soon as the fluid flow is nonparallel to the rotation axis [14]. Such forces lead to circulatory secondary flows in planes, perpendicular to the axial channel axis of a kind similar to the circulatory flows in bends.. For circular pipes it is possible to calculate these flows analytically as solutions of the Navier–Stokes obtained under

certain limiting conditions which coincide with the conditions under which the rotational particle separator operates [16]. In practical design it implies that non-parallellity of channels must be limited to specific values, to angles of inclination of a few degrees in typical cases.

5 Power consumption

The power consumption of both RPS and cyclone is investigated in detail in [1]. Energy consumption occurs mainly through the pressure drop the fluid undergoes when flowing through the apparatus. One can assume that swirl induced at the entrance (and associated radial pressure buildup) is eventually lost: the irreversible pressure loss can be taken equal to $\rho_f v_t^2$. The total energy loss can be calculated by integrating over all radial positions. For v_t and v_{ax} constant with respect to r the result is $\dot{E} = \rho_f v_t^2 Q$. Energy consumption per unit mass flow $\varepsilon = \dot{E}/(\rho_f Q)$ then amounts to $\varepsilon = v_t^2$.

The flow through the channels of the filter element of the RPS constitutes an extra pressure loss of $\Delta p_{ch} = \rho_f v_a x^2 fL/(2d_c)$. The friction factor for laminar flow in a round channel is $f = 64\mu/(\rho v_{ax} d_c)$. Here we disregard the extra pressure losses due to entrance effects, as well as blockage of channels, in practice these amount to $<10\,\%$ of the channel pressure drop. We have shown that as liquid builds up on the channel walls, shear stress exerted on the liquid is large enough to tear the liquid stream into large separable droplets downstream of the rotational particle separator [3]. We can then write for the specific energy consumption

$$\varepsilon_{ch} = \frac{S64\mu L}{\rho_f d_c^2} v_t = O(1) v_t \tag{10}$$

which in most cases can be neglected compared to the swirl term v_t^2. We can therefore conclude that the energy consumption of an RPS in first order is comparable to a cyclone with similar swirl velocity.

6 Loading

For certain applications, filter cleaning involves removal of the filter element from the apparatus and followed by cleaning an reintroduction or by replacement. For most industrial applications, however, in-situ filter cleaning is preferred, without or with limited interruption of the filtering process.

For air-jet cleaning a nozzle is fitted on top of the rotational particle separator which can move radially from inner to outer radius of the filter element (figure 12). Once the channels of the filter element become saturated with particulate material, the jet starts to blow into the channels. This can occur during normal filter operation. The radial width of the nozzle compares in size with the height of the channels, i.e. a few millimetres. Due to filter rotation, a moment will occur when the channel has passed the column of air blown from the nozzle. At this moment expansion waves start to develop from the top of the channel resulting in intense cleaning of the

channels [2]. It has been established that about 1 kg of fine particles material collected in the channels can be removed by injecting about 1 kg of compressed air at 6 bar.

As alternative to air (or other gases), cleaning of the filter element may be accomplished by periodically injecting water (or other liquids). In practice it has been established that (hot) water at pressures of 50 to 100 bar can be injected using the same nozzle as the one used for air. It offers the possibility to clean from time to time the filter very thoroughly with (hot) water, in addition to a regular air cleaning. It is particularly interesting for applications where high standards of hygiene apply.

A third method for removing particles material from the channels of the filter element is to continuously add liquid. This can occur by dispersing a spray of fine liquid particles particles are centrifuged towards the outer walls of the channels of the filter element. Here they form a liquid film which moves downwards and which carries away the other (solid) particles. The wet version of the rotational particle separator appears to be an attractive alternative to existing wet scrubbers often employed in the chemical and process industry. In contrast to wet scrubbers, in the rotational particle separator water is not injected to separate particles, but only to transport particles material being centrifuged towards the walls. This results in much lower (by up to two orders of magnitude) amounts of washing liquids [9].

In liquid applications a film builds up along the walls of the channels. The speed at which the film can be drained determines the maximum liquid load. Both theory and experiments [3] show that liquid loads up to 50 $\%_{mass}$ can be drained effectively.

7 Applications

Phase separation in centrifugal fields using the rotational particle separator has found its way, or is underway, to the market in various areas of application (figure 13). A multinational electronic consumer goods company has adopted the principle in an air cleaner. The device, which is sold world-wide, serves to remove air-borne particles which can cause respiratory allergic reactions to men in houses and offices.

Another application concerns the collection of powders and particles from gases in food and pharmaceutical processes. A specific advantage in this area is the possibility to fabricate the entire apparatus of stainless steel. It enables to meet strong conditions on hygiene and cleaning. A design has been shown in figure 11. The rotating element has been integrated in a cyclone. The cyclone acts as a pre-separator in which the gas is filtered from course particles material prior to entrance in the separation element. The cyclone also serves as a pre-swirler within which the gas is brought in rotation before entering the rotating separation element. An impeller is fitted on the downstream side of the filter element. Here, the gas is brought to the desired pressure.

It avoids the necessity of installing a separate fan. This to compensate for the pressure loss incurred in the separation device. Moreover, the over-pressure in the exit chamber ensures that only clean air flows through the gap between rotating filter element and housing from exit chamber to inlet chamber/cyclone, instead of

unfiltered air moving vice versa. On top of the device air nozzles are placed by which periodically material collected in the channels is blown towards the cyclone where it is collected in the cyclone outlet. Blowing occurs during normal operation of the filtering process, without stopping flow and rotation.

The device of the rotational particle separator can be made heat-resistant allowing temperatures up to 500 C. It has induced application of filtering hot gases of small and medium sized coal and wood combustion and gasification installations. Another feature is the capability to separate solid and liquid particles material simultaneously. It has led to the development of units suited for the filtering of polluted and misty intake air of land-based gas turbines for power generation.

In a more recent development the filter element is combined with a multistage pump to coalesce micron-sized oil droplets to over 30 times their original size [10]. Together with the water, the large droplets leave the coalescing pump to be separated in a conventional separator placed downstream.

8 Condensed Rotational Separation: a compact and energy efficient process for gas-gas separation

The RPS facilitates various kinds of innovations in the process industry. An example is the process of condensed rotational separation [8]. In this process components of a gas-gas mixture are condensed by fast reduction of temperature and pressure. The resulting mist of micron-sized droplets is removed by the RPS. Applications foreseen are: upgrading of contaminated sour gas fields [8], removal of CO2 from flue gases of coal fired power stations [16] and separation of heavy fractions from natural gas. Core of all these applications is the RPS, designed as a compact mist and aerosol catcher. It is discussed in more detail in section 9 below.

9 RPS Gas scrubber

The introduction of the RPS as a gas scrubbers in large volume applications [6] presented a number of new design issues, the most important being the behaviour under high pressure and the ability to cope with large liquid loads. As it is known that centrifugal separation is process that is sensitive to design details that are easily overlooked in CFD simulations, a visually accessible industrial scale prototype has been built before taking the step to a field test. The prototype was connected to an atmospheric test rig with water and air as working fluids. The test setup approximately models a 24 m3/s (80 MMscf/d) equivalent installation on a natural gas well. The design is suited for large liquid loads and is schematically depicted in figure 15.

Gas containing a mist of droplets enters the unit via a tangential inlet. First coarse droplets (larger than 10 micrometer) are separated in the pre-separator section. The pre-separator acts as a cyclon and collects the droplets in a stationary volute. This liquid leaves via a tangentially connected exit.

The gas stream, containing the remaining mist of mainly micron-sized droplets,

enters the rotating element. In the design point the rotating element can be driven by the impulse of the rotating flow. An external drive is can optionally be added to be able to control the rotating speed independent of the incoming flow. While traveling in the axial direction through the rotating channels, the droplets are driven to the channel walls by centrifugal force. On the walls the mist droplets coagulate into a thin fillm. The rotating element thus acts as a droplet coalescer. For optimal film behavior and minimal pressure drop the flow direction through the element is downward. Due to gravitational and shear forces, the film is forced out of the channels.

At the end of the channels the film breaks up into droplets of typically 50 micrometer. The outer wall of the rotating element extends in the axial direction beyond the end of the channels. This ensures that the solid body rotation of the gas stream leaving the element is maintained. Droplets that break of at the end of the channels are centrifugally separated from the gas in this rotating field, and collected in a film on the rotating outer wall.

Downstream of the element the post-separator section is entered, where the liquid is actually separated from the gas stream. The liquid film leaves the gas stream at the end of the extended outer wall of the rotating element towards a non-rotating collection volute. The liquid still contains significant momentum, which drives a standing film within the stationary volute. Via a tangentially connected large diameter exit the liquid leaves towards a collection vessel. The inner wall of the collection volute keeps the liquid separated from the product gas flow. This wall prevents re-entrainment of liquid due to splashing in the post-separator.

The RPS is designed to minimize any complexities involving rotation. This is achieved by containing all rotating parts, including bearings, in a pressure resistant pipe. There are no rotating shafts piercing through the wall needing rotating seals. If an external drive is needed then this happens through a magnetic coupling. Furthermore the rotating element is simple and straightforward of design implying low mechanical stresses. One can easily design for a continuous lifetime of ten years or longer

After assessing that the RPS performed to expectations regarding separation efficiency and liquid removal [11] the test rig was modified to simulate the behaviour at higher Reynolds numbers. It is known that non-rotating pipe-flow becomes becomes turbulent due to finite amplitude disturbances for bulk Reynolds numbers $Re > 2000$. However, sufficient rotation causes the flow to become unstable against infinitesimal disturbances already at $Re = 83$ [15]. Therefore, rotating pipe flow is characterized by two Reynolds numbers: the usual bulk Reynolds number $Re = v_{ax} d_c \rho_f / \mu$ and an additional rotation Reynolds number $RR = \Omega d_c^{\,2} \rho_f / 4\mu$ which comprises the rotation rate Ω (rad/s), but is independent of the distance to the rotation axis. It should be realized that, although these conditions are sufficient for the onset of instabilities, they need not correspond to the transition to turbulence.

An important implication of applying the RPS under pressure is a high gas density,

going with large Reynolds numbers. Since our laboratory test setup operates with air at atmospheric pressure, we used an extra large channel diameter to achieve a higher Reynolds number. Since the channel length to diameter ratio was kept constant, the test unit had to be lengthened as well. Figure 16 shows a measurement result, obtained using the method explained in section 3. It can be concluded that sufficient separation is achieved, also in the unstable/turbulent regime. Compared to laminar flow d_{p50} does not change, while the right hand side of the curve drops only slightly, conform DNS simulations. We can now safely release the earlier restriction of purely laminar flow.

Often the performance of a gas scrubber is presented in the form of a sizing or load factor K as used in the Sounders-Brown equation. The required gas scrubber area (footprint) can than be calculated from

$$A = \frac{Q_A}{K}\sqrt{\frac{\rho_l}{\rho_l - \rho_g}} \tag{11}$$

The load factor K is a direct measure for the required footprint of the installation and has the unit of velocity. In figure 17 we have compared the best practice of scrubbers with that of a RPS. Only under atmospheric pressure and a d_{p50} of 3 micrometer is the size of a cyclone deck comparable to that of a RPS. Otherwise the RPS is significantly smaller and capable of separating particles in the submicron range. Application of the RPS is thus particularly advantageous when working at elevated pressures and large flows as is the case in the process of condensed rotational separation (section 8).

10 Concluding remarks

Main features of the rotational particle separator as a new device for separating micron sized particles or droplets from carrier fluids have been presented.

Performance indicators as size of of particles separated, energy consumption per unit throughflow and size of the unit compare favorably with conventional methods based on vane separators and cyclones.

The RPS facilitates various innovations in process industry. An example is the compact and energy efficient process of condensed rotational separation.

Acknowledgment

The authors wish to thank Romico Hold for access to proprietary knowledge regarding the RPS and related processes

References

[1] R.J.E. van Wissen, J.J.H. Brouwers, M. Golombok, In-line centrifugal separation of dispersed phases, AIChE Journal, 53(2), 374-380, (2007)

[2] J.J.H. Brouwers, Particle collection efficiency of the rotational particle separator, Powder Technology 92 (1997) 89-99.

[3] G.P. Willems, Condensed rotational cleaning of natural gas, PhD. Thesis, 2009, TUE

[4] H.G. Houghton and W.H. Radford , Measurements on eliminators and the development of a new type for use at high gas velocities. Transactions of the American Chemical Engineers 35 (1939), pp. 427–433

[5] Kemenade HP van, Mondt E, Hendriks AJAM, Verbeek PHJ. Liquid-Phase Separation with the Rotational Particle Separator, Chem. Eng. Techn. 2003;26(11):1176-1183

[6] Mondt E, Kemenade HP van, Schook R. Operating performance of a naturally driven Rotational Particle Separator, Chem. Eng. Techn. 2006;29(3):375-383

[7] Brouwers JJH. Phase separation in centrifugal fields with emphasis on the rotational separator. Exp Therm Fluid Sci; 2002;26: 325-334.

[8] Kemenade HP van, Brouwers JJH, Benthum RJ. Condensed Rotational Separation, 2011 AFS annual conference, May 10-12, Louisville, USA

[9] E. Mondt, H.P. van Kemenade, J.J.H. Brouwers, E.A. Bramer, Rotating Sorbent Reactor, in 3rd International Symposium on Two Phase Flow Modelling and Experimentation; Editors: G.P. Celata, P. Di Marco, A Mariani, R.K. Shah, Pisa, Italy

[10] Liebrand H, Wals E. New Technology to improve the performance of produced water separation systems, In: 9th Produced Water Workshop, Aberdeen, May 18th-19th

[11] Willems GP, Kroes JP, Golombok M, Esch BPM van, Kemenade HP van, Brouwers JJH. Performance of a Novel Rotating Gas-Liquid Separator, J. Fluid Eng. 2010;132(3):031301

[12] Kuerten JGM, Esch BPM van, Kemenade HP van, Brouwers JJH. The effect of turbulence on the efficiency of the rotational phase separator, Int. J. Heat Fluid Flow 2007;28:630-637

[13] Esch BPM van, Kuerten JGM. Direct numerical simulation of the motion of particles in rotating pipe flow, J. Turbulence 2008;9(4):1-17, (2008)

[14] J.J.H. Brouwers, Secondary Flows and Particle Centrifugation in Slightly Tilted Rotating Pipes, Applied Scientific Research 55: 95-105, 1995.

[15] Mackrodt, P. A. `Stability of Hagen-Poiseuille flow with superimposed rigid rotation', J. Fluid Mech. 73(1), 153--164.

[16] Kemenade, H.P. van, Benthum, R.J. van, Brouwers, J.J.H. & Golombok, M. (2011). Condensed Rotational Separation of CO2. The Clearwater Clean Coal Conference June 5 to 9, 2011, Clearwater, Florida, USA

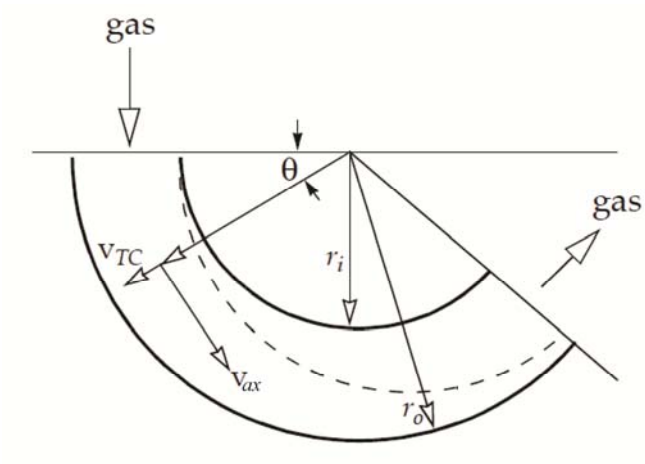

figure 1: Vane type separator

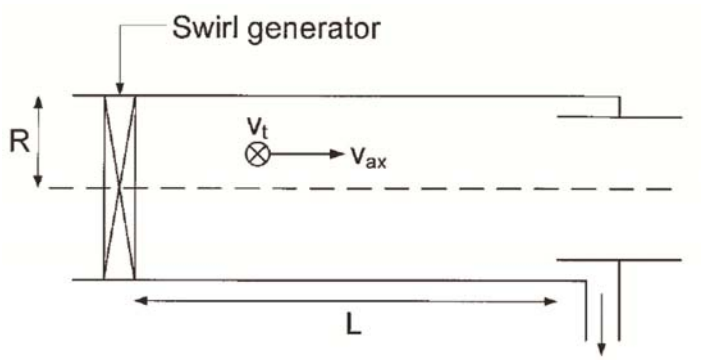

figure 2: Axial cyclone

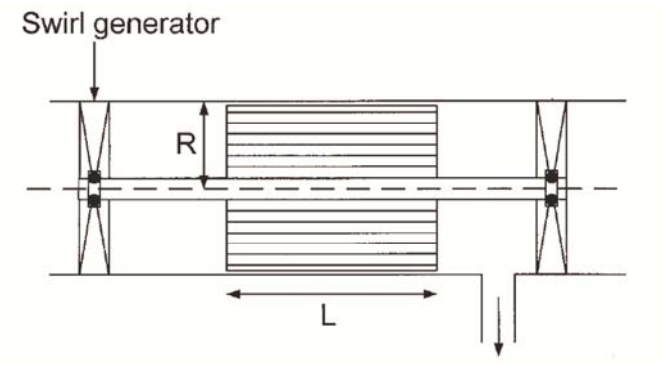

figure 3: Axial RPS

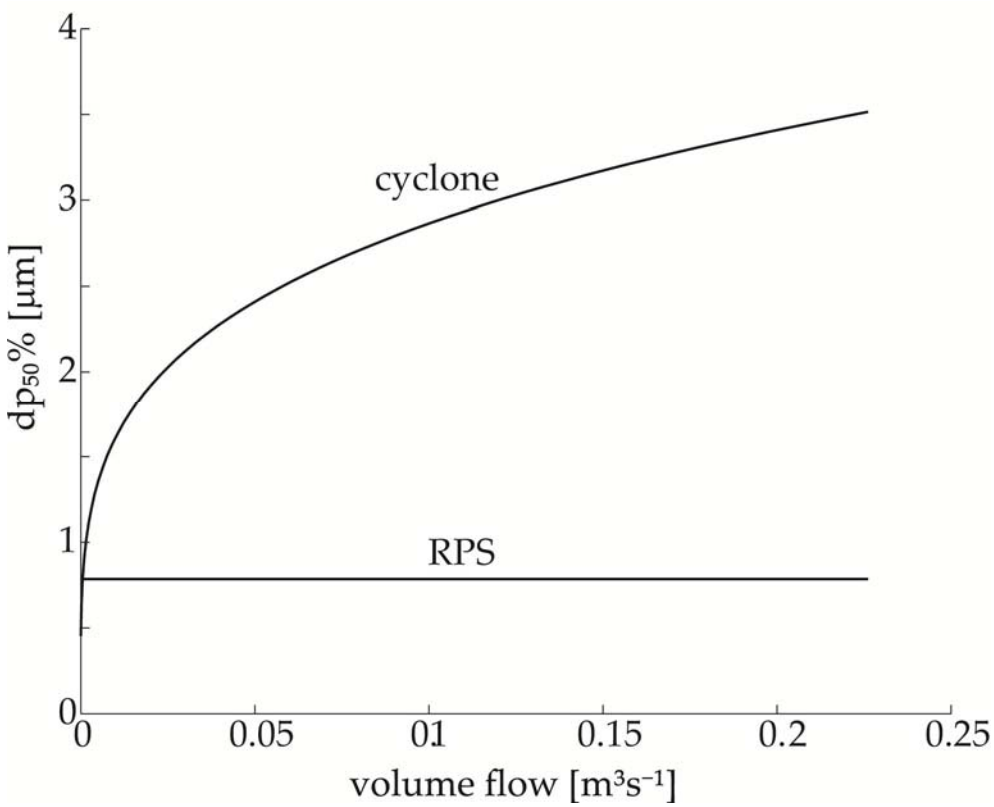

figure 4: diameter of water droplets in air separated by a cyclone and RPS as function of the volume flow under atmospheric pressure

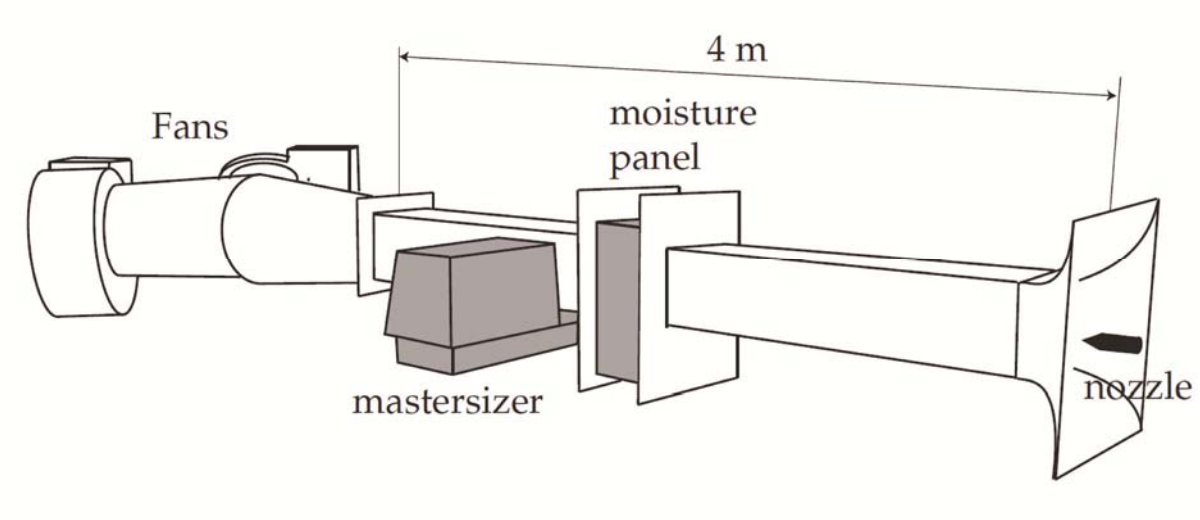

figure 5: Experimental set-up

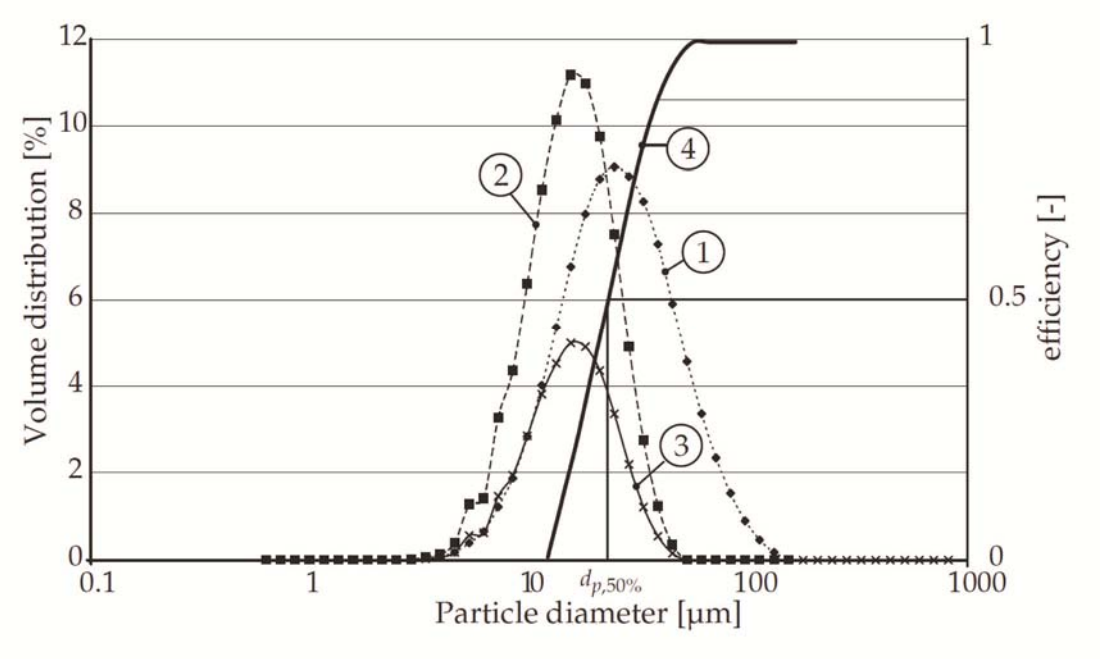

figure 6: Typical measurement result: Curves (1) to (2) are the volume distributions measured without and with separator present. Curve (3) is curve (2) scaled to (1). The efficiency curve (4) is obtained as 1-(3)/(1).

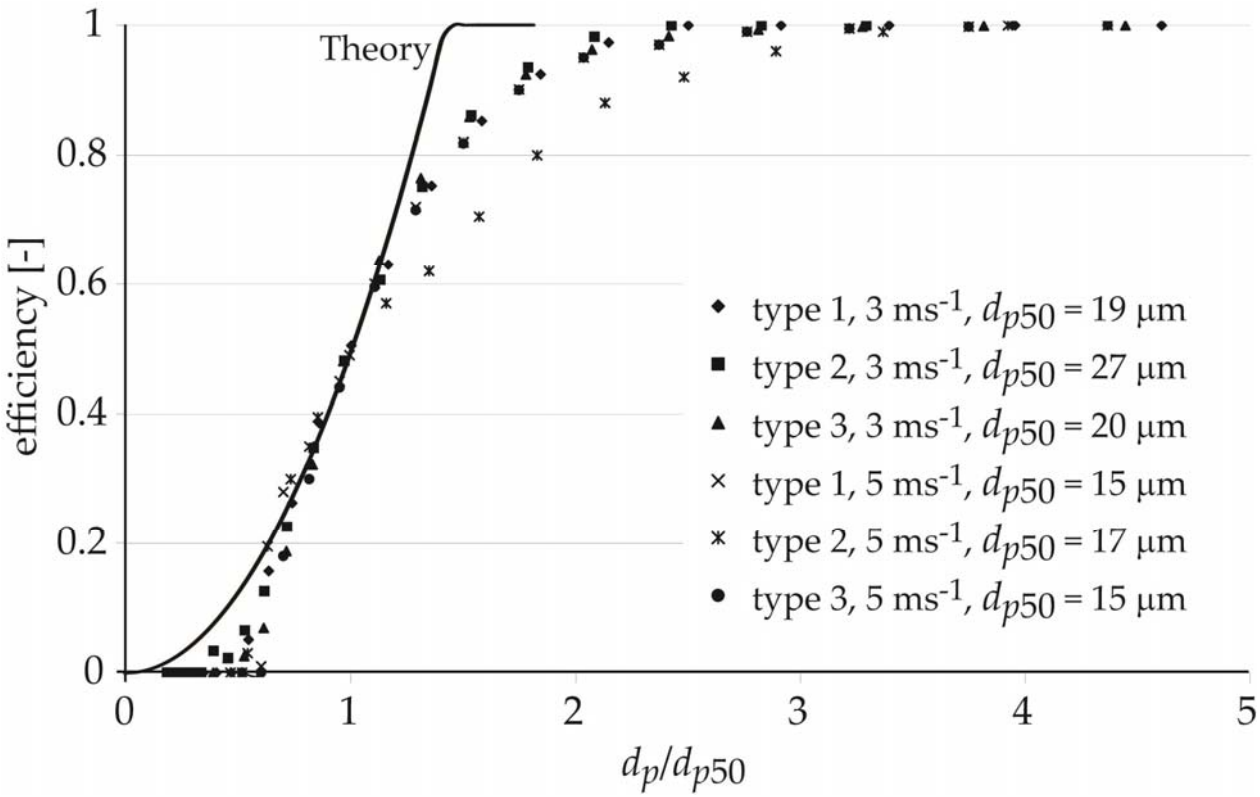

figure 7: Measured panel efficiency

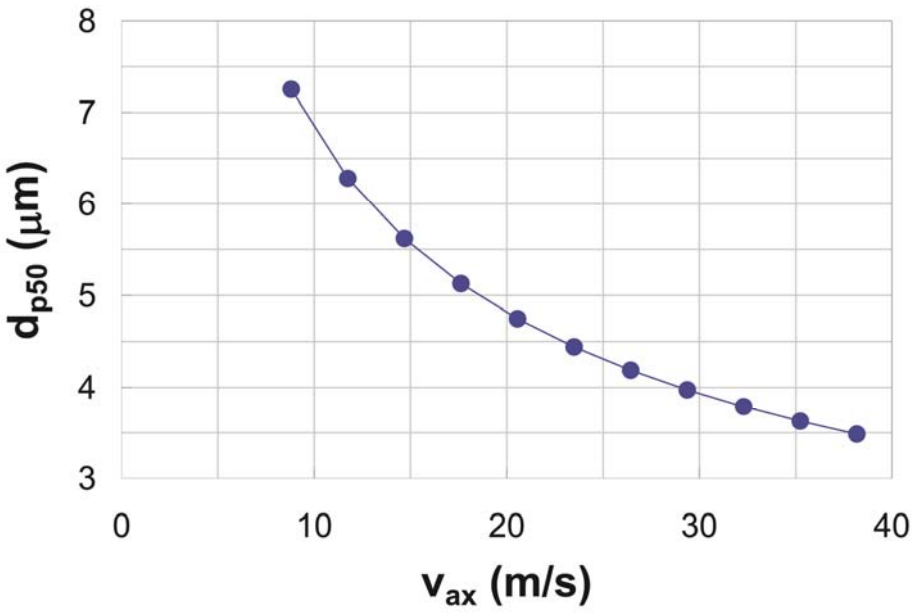

Figure 8: Axial cyclone d_{p50} as a function of mean axial velocity v_{ax}. Swirl ratio $S = v_t/v_{ax} = 1.2$ and $L/R = 5.6$.

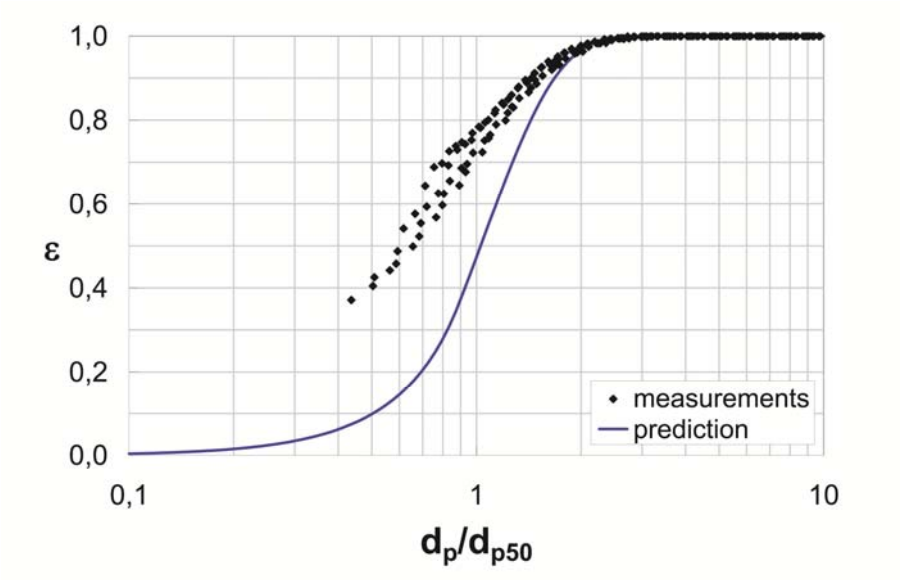

figure 9: Measured efficiency ε as a function of the particle size d_p, made nondimensionless with d_{p50}. Results below 3 micron were disregarded. Prediction is based on plug flow, and a Rankine vortex profile with core radius $0.8R$.

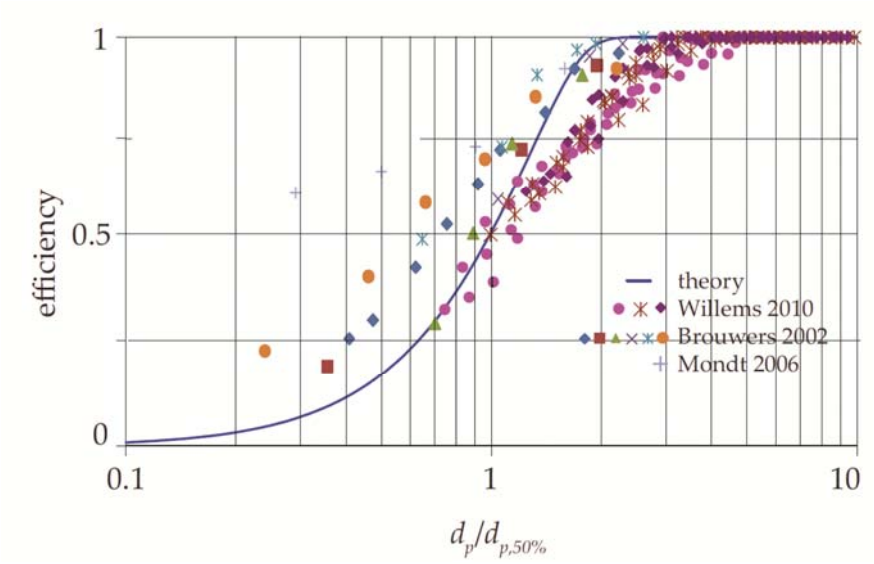

figure 10: Efficiency of the rotating particle separator.

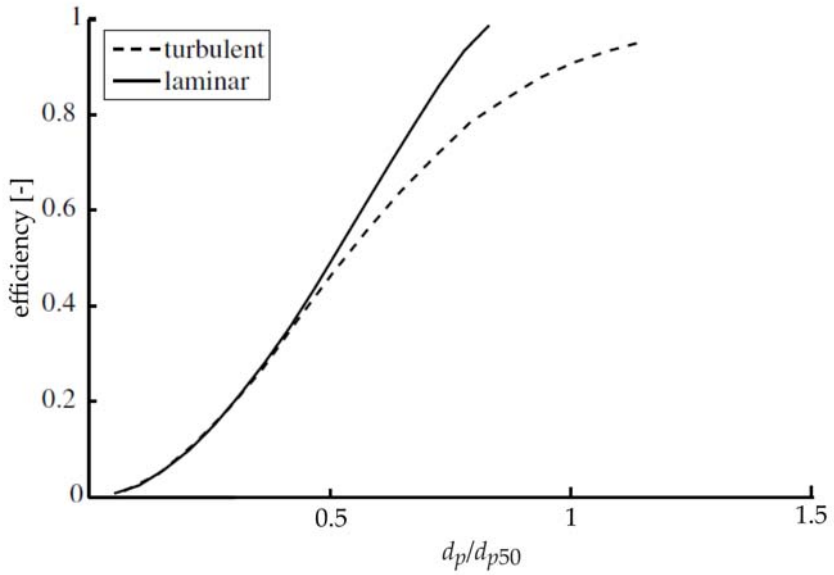

figure 11: Efficiency of the RPS for laminar and turbulent flow

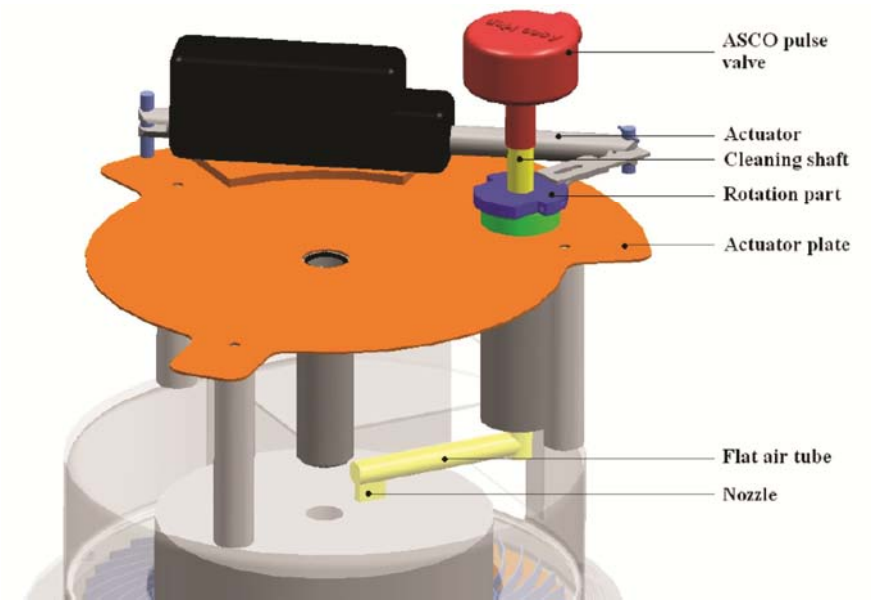

figure 12: Jet cleaning system of a RPS

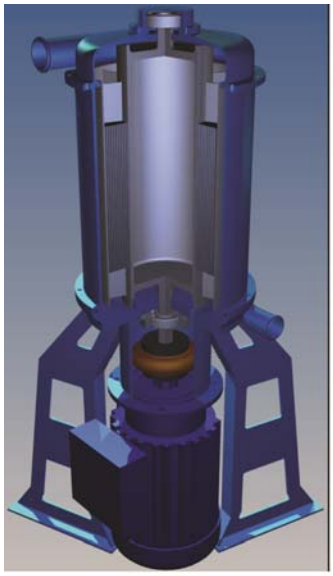

Oil/water
separation

air cleaning in
domestic applications

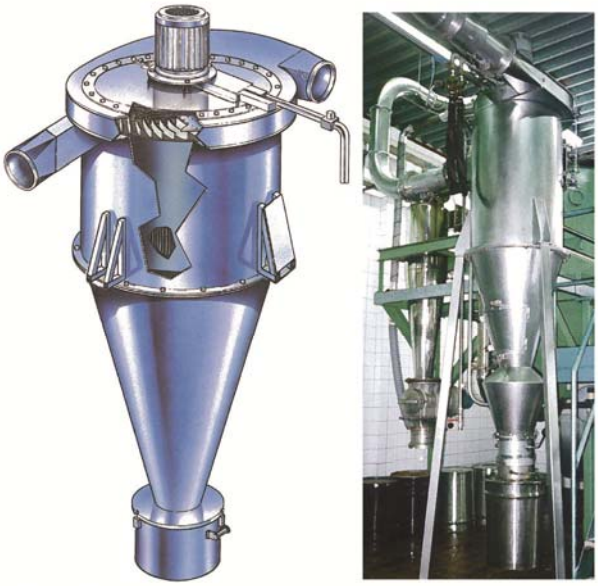

high temperature & sanitary
applications

CRS

figure 13: Application examples of the RPS

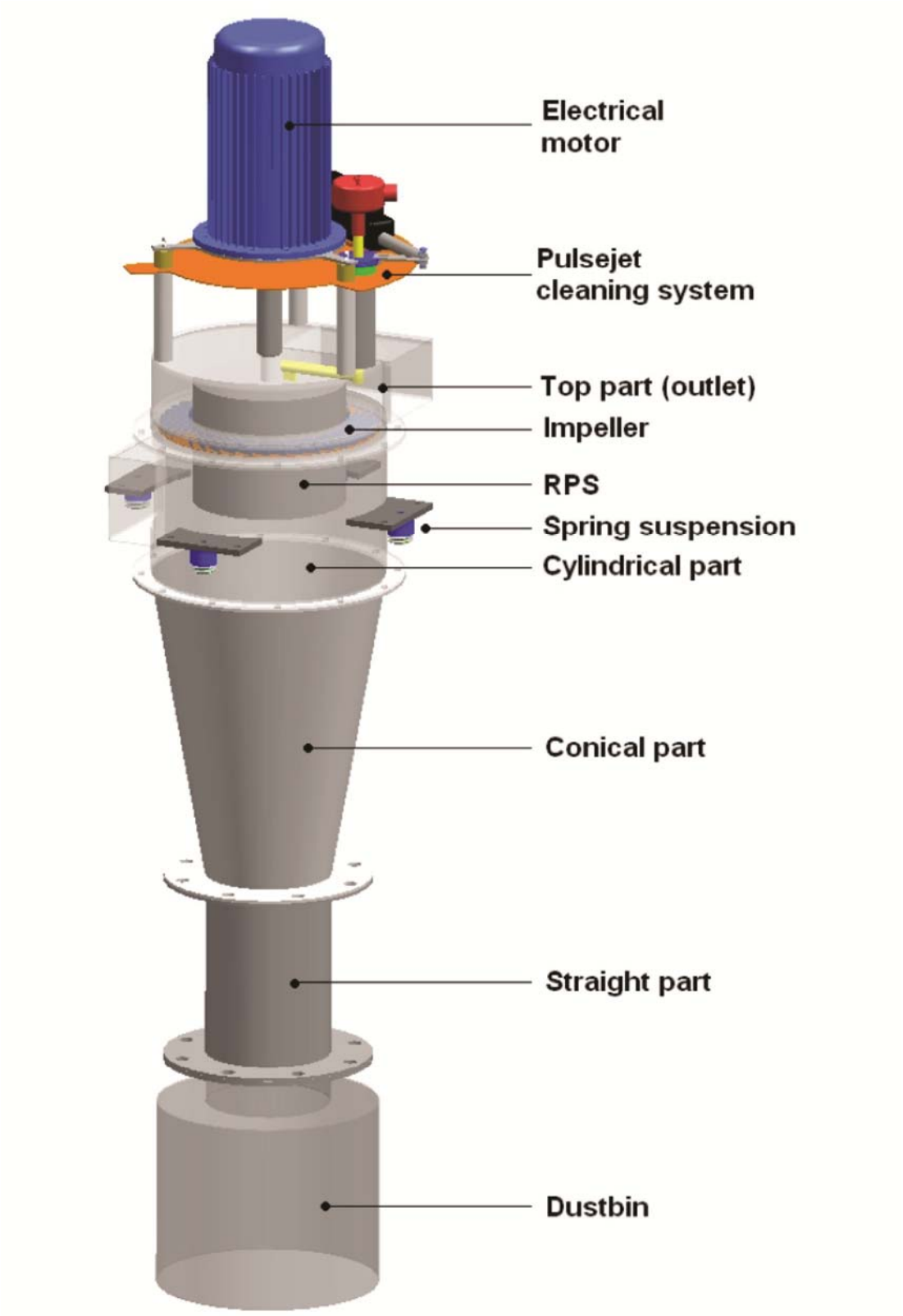

figure 14: RPS integrated with a cyclone and fan

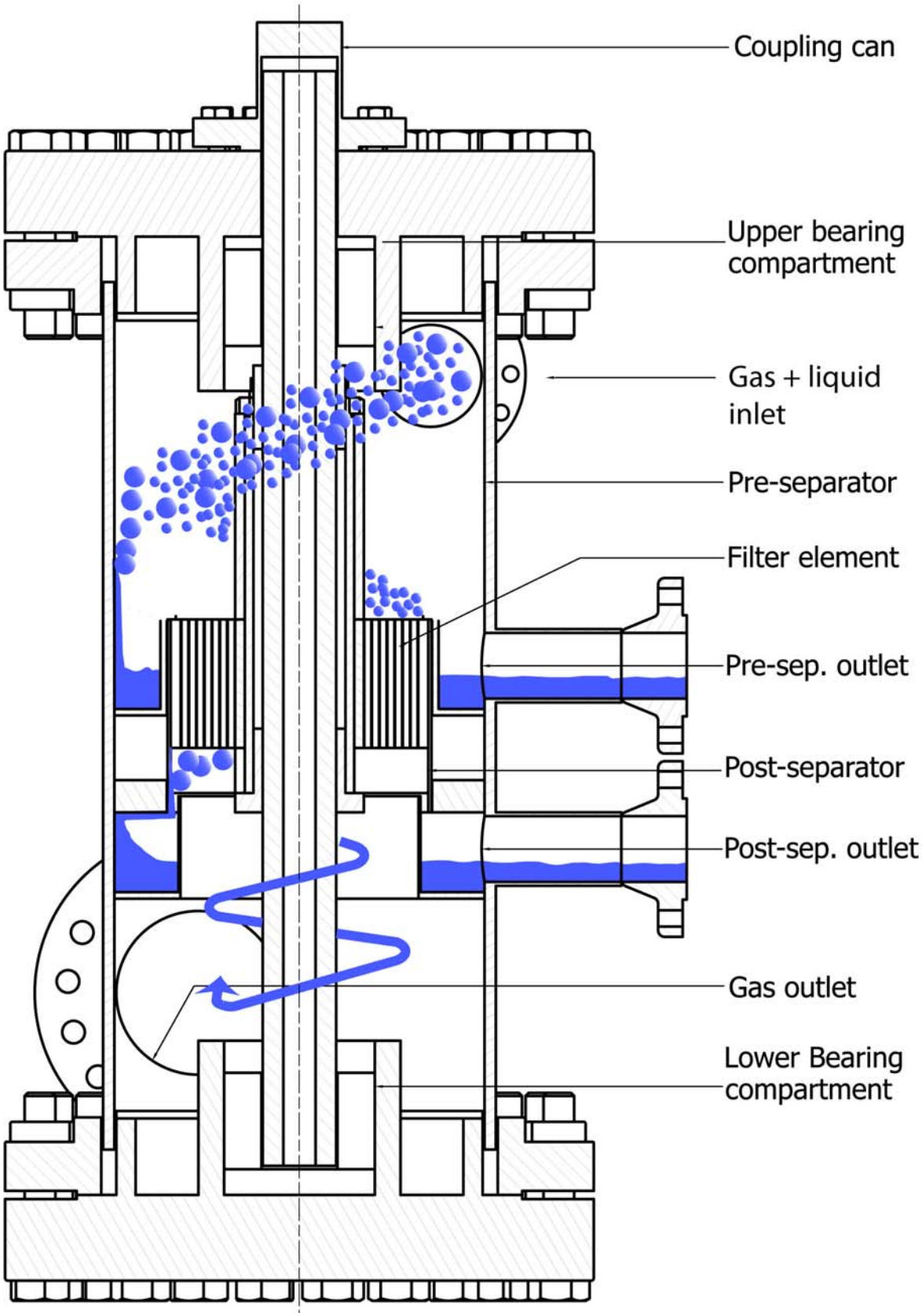

figure 15: High volume RPS mist catcher design

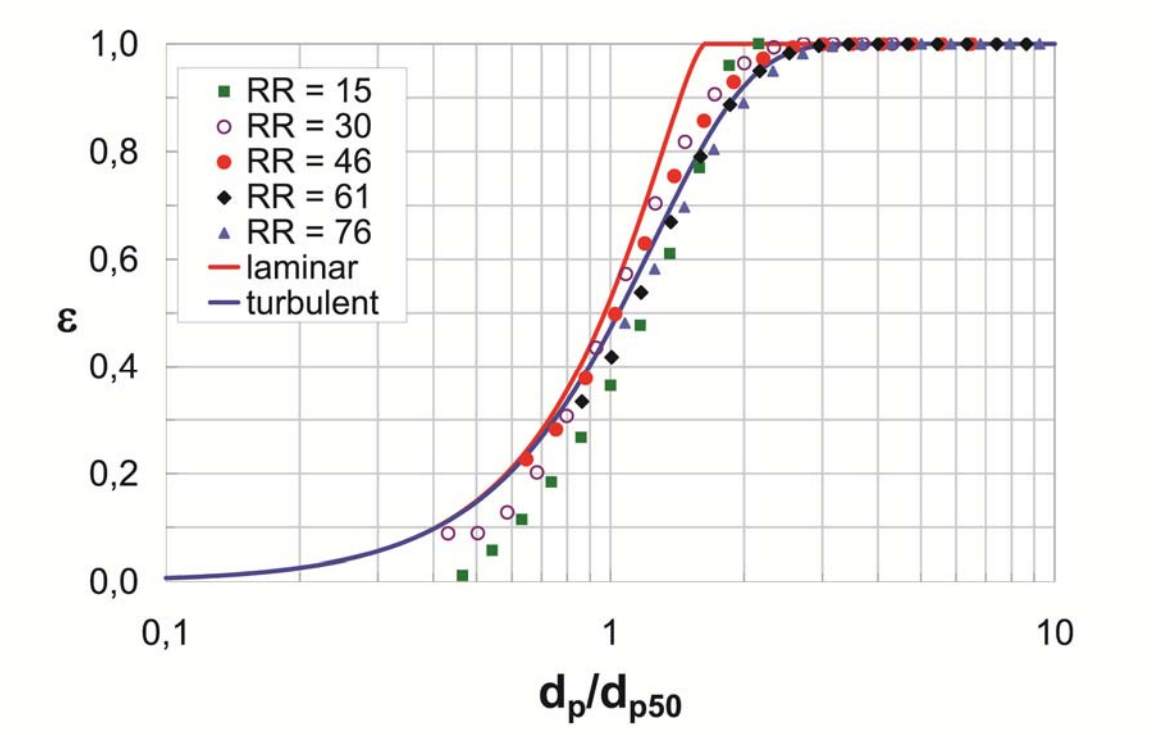

Figure 16: Efficiency of the RPS with unstable flow in the rotating channels ($Re = 1070$).

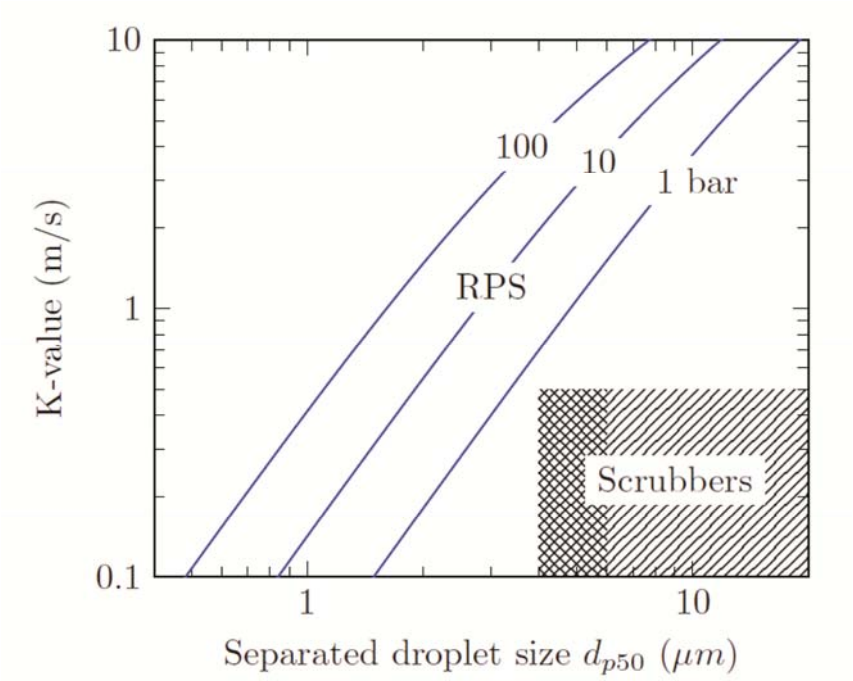

figure 17: K-values for the RPS and scrubbers. Crosshatch pattern indicates best practice using cyclone decks.